Received: 17 January 2025 | Revised: 26 May 2025 | Accepted: 5 June 2025

DOI: 10.1111/joa.70009

Journal of Anatomy | ANATOMICAL SOCIETY WILEY

ORIGINAL ARTICLE

Diversity and development of the hemibacula of croaking geckos (Sphaerodactylidae: *Aristelliger*)

Aaron H. Griffing[1,2,3] | Daniel J. Paluh[4] | Jonathan C. DeBoer[5] | Juan D. Daza[6] | Tony Gamble[3,7] | Anthony P. Russell[8] | Aaron M. Bauer[9]

[1]Department of Chemical and Biological Engineering, Princeton University, Princeton, New Jersey, USA

[2]Department of Molecular Biology, Princeton University, Princeton, New Jersey, USA

[3]Milwaukee Public Museum, Milwaukee, Wisconsin, USA

[4]Department of Biology, University of Dayton, Dayton, Ohio, USA

[5]Department of Geography, University of Nevada, Reno, Nevada, USA

[6]Department of Biological Sciences, Sam Houston State University, Huntsville, Texas, USA

[7]Department of Biological Sciences, Marquette University, Milwaukee, Wisconsin, USA

[8]Department of Biological Sciences, University of Calgary, Calgary, Alberta, Canada

[9]Department of Biology and Center for Biodiversity and Ecosystem Stewardship, Villanova University, Villanova, Pennsylvania, USA

Correspondence
Aaron H. Griffing, Department of Chemical and Biological Engineering, Princeton University, Princeton, NJ 08544, USA.
Email: ag3200@princeton.edu

Funding information
National Science Foundation, Grant/Award Number: DBI 2109344 and DBI 2209090

Abstract

Among squamates, hemipenes are known to evolve rapidly and exhibit diverse shapes, sizes, and ornamentation. Croaking geckos (*Aristelliger*) are unique among geckos in exhibiting mineralized structures (hemibacula) in their hemipenes. We here describe the gross morphology of the hemibacula of each currently recognized species of *Aristelliger*, document hemibacular histology, and report on hemibaculum development. We confirm the presence of hemibacula in all currently recognized species and demonstrate that three distinct morphologies correspond to three putative clades in the genus. Histology revealed that hemibacula are superficially similar to chondroid bone and composed of mineralized dense connective tissue covered in a thin layer of epidermis with alcian-positive cells embedded within a mineralized matrix. Additionally, we demonstrate that hemibacula do not develop until past the onset of sexual maturity and that hemibaculum length scales isometrically with body size. We hypothesize that hemibacula of *Aristelliger* develop via peramorphosis, a phenomenon also expressed in the cranial morphology of this genus. Additionally, we speculate on the functional significance of these enigmatic structures.

KEYWORDS
bacula, diaphonization, Gekkota, hemipenes, histology, reptile, squamate, μCT

1 | INTRODUCTION

Male intromittent organs of squamates (i.e., hemipenes) are diverse in shape, size, and ornamentation, thereby lending themselves to their use as characters for phylogenetic analyses (e.g., Arnold, 1986a; Böhme, 1988; Brennan & Bauer, 2017; Card & Kluge, 1995; Dowling & Savage, 1960; Keogh, 1999; Köhler et al., 2012). The hemipenes of gekkotan lizards, for example, are generally characterized by a club-shaped truncus, pedicel, and voluminous apex (Böhme, 1988; Cope, 1896). The hemipenial apices are typically bi-lobed, reflecting the hypothesized ancestral gekkotan condition (Brennan & Bauer, 2017). Surfaces of the hemipenial trunk, pedicel, and apex often exhibit variable calyculate ornamentation (Böhme, 1988). Apical epidermal ornamentation can be extremely variable, expressing, for example, as fleshy, hardened papillae (e.g., *Uroplatus*; Glaw et al., 2006) or spines (e.g. *Aprasia*, *Hemidactylus*; Brennan & Bauer, 2017; Das & Purkayastha, 2012). A further elaboration of hemipenial ornamentation is the presence of baculum-like, ostensibly "ossified" structures, called hemibacula (also known as hemipenial bones sensu Böhme, 1988; Kluge, 1982). It is important to note, however, that the presence of true bone has not previously been histologically verified in the hemibacula of squamates (Al-ma'ruf et al., 2021; Card & Kluge, 1995; Werner, 1988). Mineralized surface ornamentation of hemipenes has been reported in several squamate lineages (e.g., Cadle, 2011; Glaw et al., 1999; Nunes et al., 2014); however, hemibacula appear to be distinct from surface ornamentation because they are embedded deep within the hemipenes as opposed to being restricted to the integument of the outside of the everted hemipenes (Card & Kluge, 1995; Kluge, 1982). Hemibacula are a product of convergent evolution, having only been reported in three separate squamate lineages: varanid lizards, the gekkonid gecko *Uroplatus lineatus*, and four species of the sphaerodactylid gecko genus *Aristelliger* (Böhme, 1988; Branch, 1982; Card & Kluge, 1995; Kluge, 1982; Rösler & Böhme, 2006; Russell, 1977; Shea & Reddacliff, 1986; Smith, 1935; Werner, 1988). Hemibacula were reported in the sphaerodactylid *Teratoscincus bedriagai* by Jahed-Haghshenas and Hojati (2015); however, we consider this observation to be doubtful and were unable to confirm their presence in cleared-and-stained male specimens of *T. bedriagai* (MVZ 236999–7002). Instead, these specimens revealed no obvious mineralized or cartilaginous elements within the adult hemipenes but only the presence of post-cloacal bones which are subcutaneous bony elements associated with the cloacal sacs (Russell et al., 2016). Within the Sphaerodactylidae, such post-cloacal bones are only known to be present in two genera: *Teratoscincus* and *Euleptes* (Russell et al., 2016). The hemibacula of varanids are generally characterized by apical structures, with one to three individual elements per hemipenis that express varying degrees of mediolateral element size and shape asymmetry (Böhme, 1988; Card & Kluge, 1995; Shea & Reddacliff, 1986). The hemibacula of the gekkonid gecko *U. lineatus* are characterized by a single smooth, thick, two-pronged element per hemipenial lobe, connected to a thick retractor muscle (Rösler & Böhme, 2006). Whether these elements are ossified or mineralized is unknown. The lateral and medial processes of each hemibaculum are of unequal length (4 and 3 mm, respectively), with the lateral process being recurved and visible from the apex of the hemipenis lobe. The hemibacula of *Aristelliger* are characterized by one to two highly denticulate elements per hemipenial lobe (Figure 1). At least one such element is scimitar-shaped (hereafter referred to as "element I"), appearing to protrude through the apex of the hemipenis lobe, with the outer surface of the curve exhibiting tooth-like projections. If there is a second element, it is two-pronged (hereafter referred to as "element II") with a lateral process extending more distally than the medial one (Kluge, 1982; Rösler & Böhme, 2006).

Since their discovery, the hemibacula of *Aristelliger* have been described only briefly, based on cleared-and-stained specimens of *A. expectatus* and *A. praesignis*, and fluid-preserved *A. georgeensis* (Kluge, 1982; Rösler & Böhme, 2006). Hemibacula were also illustrated radiographically in *A. lar* by Russell (1977) but were erroneously identified as post-cloacal bones. Despite a rich body of literature describing hemipenial morphologies, the novel denticulate hemibacula of *Aristelliger* have been largely overlooked. Furthermore, ontogenetic variation in hemipenial morphologies has rarely been considered (Böhme, 1988; De Lima et al., 2019). In this study, we investigate the diversity of hemibacula in each currently recognized species of *Aristelliger*, comment on their implications for the systematics of this genus and the evolution of its reproductive anatomy, and explore their tissue composition and ontogenetic variation.

2 | METHODS

We compared hemibacular morphology between *Aristelliger barbouri*, *A. cochranae*, *A. expectatus*, *A. georgeensis*, *A. hechti*, *A. lar*, *A. nelsoni*, *A. praesignis*, and *A. reyesi* using cleared and stained specimens, fluid-preserved specimens imaged using microcomputed tomography (μCT), and radiographed specimens (Table 1). We examined 17 individuals of *A. praesignis*, all collected within a 10-km radius in St. Andrew Parish, Jamaica during June 2016, to assess ontogenetic development of, and intraspecific variation in, hemibacula. Specimens were collected with permission from the Jamaica National Environment & Planning Agency (Permit Ref. #18/27). For specimens we field-collected, hemipenes were everted and inflated following euthanasia (Conroy et al., 2009) by administering a postcloacal injection of neutral-buffered formalin and ligating the base of each individual hemipenis for the duration of fixation (Simmons, 2015). We used snout–vent length (SVL) as a proxy for ontogenetic age (Table 1). For both μCT data and cleared and stained specimens, we measured the lengths of hemibacula using curved measurements in Fiji v2.0.0 (Schindelin et al., 2012). To investigate the scaling of hemibacula with ontogenetic stage, we log-transformed SVL and hemibacula length measurements and performed linear regressions. Slopes of each regression were compared to a slope = 1 (i.e. isometry) using a single-tailed *t*-test. In

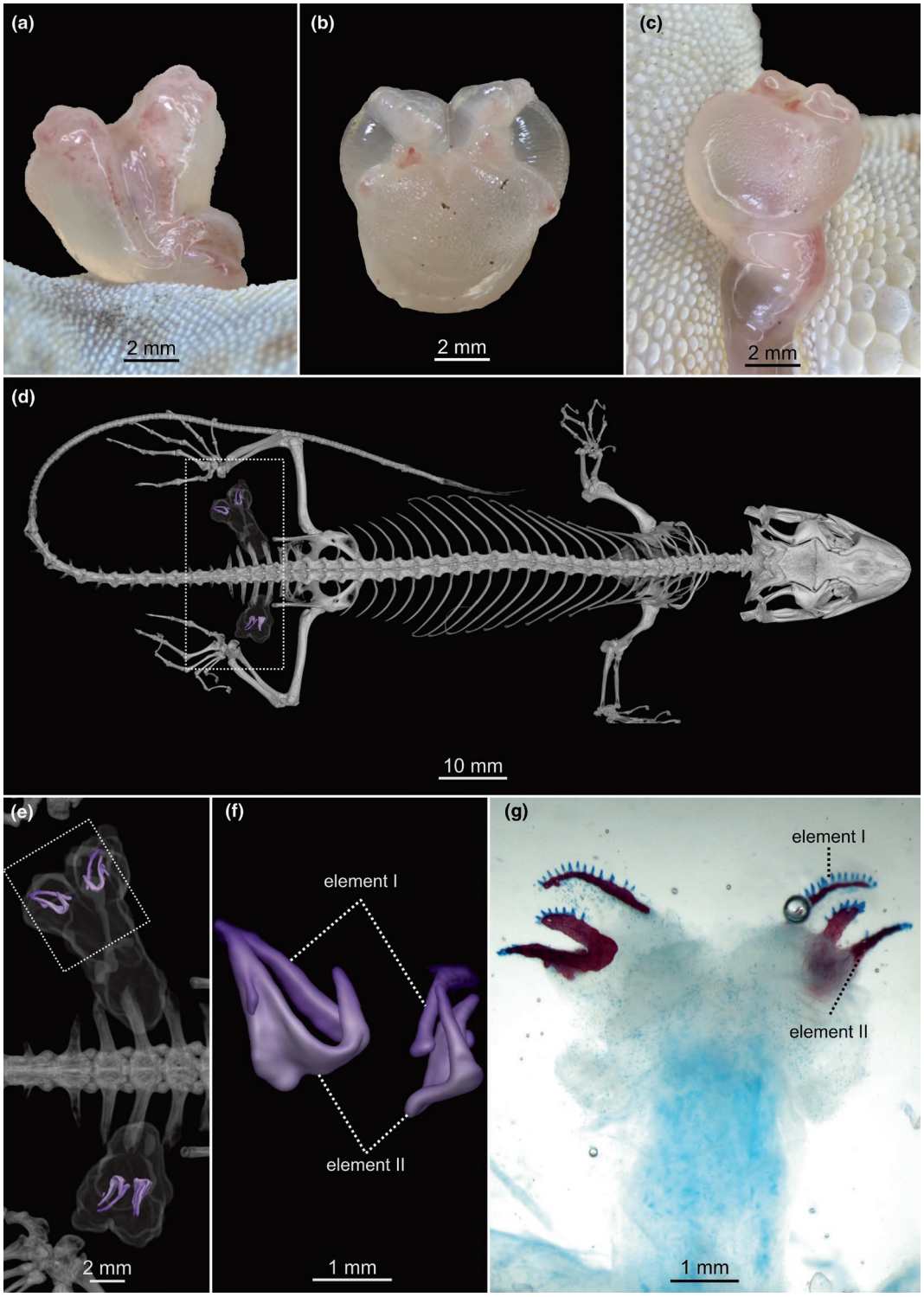

FIGURE 1 Hemibacular morphology of the everted hemipenes of large-bodied *Aristelliger*. (a–c) brightfield images of a hemipenis of *Aristelliger lar* (TG 3883) in sulcal (a), apical (b), and asulcal (c) views. (d–f) μCT images of the hemibacula of *Aristelliger georgeensis* (UF-H-126373) in sulcal (d) and asulcal views (e, f). Hemibacula are illustrated in purple. (g) A cleared and stained everted hemipenis of *Aristelliger praesignis* (MCZ-R-194579) illustrating that the hemibacula possess mineralized tissue (red) and chondroitin sulfate (dark blue).

addition to whole-mount specimens, we examined the histological structure of the hemibacula of the hemipenis of a captive-born *A. lar* (TG 3883). Acronyms for institutional collections are as follows: AMNH, American Museum of Natural History, New York, New York, USA; KU, University of Kansas Natural History Museum, Lawrence, Kansas, USA; MCZ, Harvard Museum of Comparative Zoology, Harvard University, Cambridge, Massachusetts, USA; MVZ, Museum of Vertebrate Zoology, University of California at Berkeley, Berkeley, California, USA; NHMJ, Natural History Museum of Jamaica, Kingston, Jamaica; USNM and NMNH, National Museum

TABLE 1 *Aristelliger* specimens examined in this study and the attributes of their hemibacula. Specimen preparation (Prep.): Cleared-and-stained (C/S); radiographed (X-ray); histological sectioning (histo); and microcomputed tomography (μCT) specimens. Hemipenis status (Status): Everted (E); partially everted (PE); and inverted (I). Average length measurements of element I (EI), the lateral process of element II (EIIL), and medial process of element II (EIIM). "—" corresponds to an absence of data.

Specimen ID	Species	Prep.	SVL (mm)	Status	EI (mm)	EIIL (mm)	EIIM (mm)
AMNH 45794	*A. barbouri*	μCT	43.7	I	0.72	—	—
AMNH 45820	*A. barbouri*	μCT	36.0	E	0.81	—	—
AMNH 45795	*A. barbouri*	μCT	38.8	PE	—	—	—
KU H-228585	*A. cochranae*	C/S	58.2	I	1.20	—	—
UF H-21858	*A. cochranae*	μCT	43.8	E	0.95	—	—
UF H-126372	*A. expectatus*	μCT	46.5	E	0.57	—	—
KU H-070036	*A. georgeensis*	C/S	88.1	PE	1.74	1.55	1.00
KU H-070027	*A. georgeensis*	C/S	95.6	E	1.85	1.86	1.10
UF H-126373	*A. georgeensis*	μCT	89.7	E	2.41	2.30	1.18
KU H-228757	*A. hechti*	C/S	86.4	E	1.62	1.81	—
KU H-228752	*A. hechti*	μCT	69.3	E	1.47	1.56	—
USNM 260002	*A. lar*	X-ray	102.4	E	2.07	2.47	—
USNM 260003	*A. lar*	X-ray	102.7	PE	1.87	1.71	—
KU H-228785	*A. lar*	C/S	129.9	E	1.97	2.70	—
UF H-186878	*A. lar*	μCT	98.2	E	2.02	2.40	—
TG 3883	*A. lar*	histo	98.4	E	—	—	—
NMNH 252332	*A. praesignis*	C/S	46.4	E	1.68	1.70	1.19
KU H-228995	*A. praesignis*	C/S	87.5	I	1.92	1.36	1.28
MCZ R-194590	*A. praesignis*	C/S	52.3	E	0	0	0
MCZ R-194581	*A. praesignis*	C/S	57.9	E	0	0	0
MCZ R-194566	*A. praesignis*	C/S	60.3	E	1.25	1.30	0.98
MCZ R-194588	*A. praesignis*	C/S	60.8	E	1.35	0.87	0
MCZ R-194575	*A. praesignis*	C/S	74.9	E	1.59	1.18	0.92
MCZ R-194583	*A. praesignis*	C/S	74.9	E	1.36	1.20	0.74
NHMJ R-283	*A. praesignis*	C/S	78.5	E	1.53	1.28	1.10
MCZ R-194579	*A. praesignis*	C/S	83.2	E	1.58	1.58	1.21
MCZ R-194584	*A. praesignis*	C/S	83.5	E	1.51	1.10	1.18
MCZ R-194576	*A. praesignis*	C/S	86.5	E	1.14	1.34	0.87
MCZ R-194595	*A. praesignis*	C/S	88.2	E	1.73	1.23	2.37
MCZ R-194597	*A. praesignis*	C/S	88.2	E	1.54	1.35	1.55
MCZ R-194586	*A. praesignis*	C/S	89.6	E	1.44	0.712	0.93
MCZ R-194592	*A. praesignis*	C/S	96.5	E	1.72	1.24	1.08
MCZ R-194591	*A. praesignis*	C/S	96.9	E	1.73	1.21	1.15
MCZ R-194598	*A. praesignis*	C/S	97.4	E	1.79	1.29	1.07
MCZ R-194594	*A. praesignis*	C/S	97.9	E	1.89	1.64	1.35
UF H-21756	*A. praesignis*	μCT	73.1	I	1.46	1.50	1.20
USNM 494659	*A. nelsoni*	μCT	78.4	E	1.57	1.94	1.24
USNM 494664	*A. nelsoni*	X-ray	77.9	E	1.61	1.58	1.08
UF H-188677	*A. reyesi*	μCT	55.2	I	1.02	—	—

of Natural History, Smithsonian Institution, Washington DC, USA; TG, Collection of Tony Gamble, Marquette University, Milwaukee WI, USA; UF, Florida Museum of Natural History, Gainesville, Florida, USA.

We employed radiographs and images of cleared and stained specimens assembled as part of a previous study (Griffing et al., 2018). For clearing and staining, we followed the protocol of Bauer (1986) modified from Wassersug (1976) and Hanken and Wassersug (1981).

Briefly, we cleared soft tissue, stained mineralized tissue with alizarin red S, and stained for proteoglycans and glycosaminoglycans (including chondroitin sulfate) with Alcian Blue. Chondroitin sulfate is a major component of connective tissues, being most commonly employed as a marker for cartilage (Lindahl & Hook, 1978; Theoharides et al., 2000). We visualized and photographed ventral views of the cloacal region of cleared and stained specimens using a Nikon SMZ1000 stereomicroscope and a Nikon Digital Sight microscope camera (Villanova University). We deposited images of all cleared and stained hemipenes in FigShare. We obtained digital radiographs at the Smithsonian National Museum of Natural History using a KevexTM PXS10-16 W X-ray source and Varian Amorphous Silicon Digital X-Ray Detector PaxScan H4030R (130 kV, 81 μA). For histology, the specimen was fixed in 10% neutral-buffered formalin with the hemipenes everted and stored in 70% ethanol. After removing a hemipenis and rehydrating the specimen, we decalcified it by immersion in 10% formic acid for 6 h. We embedded the hemipenis in OCT Compound (Tissue-Tek) and generated 12 μm serial histosections using a Leica CM3050S cryostat. To aid in visualization of mineralized tissue (red) and cartilage (blue), we stained sections using a Hall-Brundt Quadruple stain (HBQ; Hall, 1986) using the modifications of Kerney et al. (2009). We visualized and photographed histosections using a Nikon Eclipse Ni-E compound microscope with Nikon DS-Qi2 camera (Princeton University).

We performed high-resolution X-ray computed tomography scanning using a GE v|tome|x M 240 system at the Nanoscale Research Facility (University of Florida, Gainesville, USA). We conducted scans using a 180 kv X-ray tube containing a diamond-tungsten target, with the voltage and the current adjusted to maximize the absorption range for each specimen. We processed the raw X-ray data using GE's datos|x v2.3 software, producing tomogram and volume files. We imported these microCT volume files into VG StudioMax v3.5 (Volume Graphics, Heidelberg, Germany) and isolated the skeleton and mineralized hemipenial structures using the suite of segmentation tools in VG StudioMax. Linear measurements were recorded using the polyline length tool in VG StudioMax. We deposited image stacks (TIFF) and 3D mesh files (STL) in MorphoSource (Project ID: 0000C1044).

3 | RESULTS

3.1 | Characterization of hemibacula

We confirmed the presence of hemibacula in the hemipenes of all nine species we examined. Cleared-and-stained female specimens of *Aristelliger praesignis* did not exhibit any noticeable mineralized tissues in the cloacal region. The hemipenes of *A. barbouri*, *A. cochranae*, *A. expectatus*, and *A. rayesi* (Subgenus *Aristelligella*) possess a single, scimitar-shaped element I per hemipenial lobe (Figure 2). In our sample, average lengths of these elements ranged from 0.57–1.20 mm (Table 1). In these four species, the hemibacula are proximally bulbous and taper distally (Figure 2). We examined only a single cleared-and-stained specimen belonging to this group (*A. cochranae*; KU H-228585), which was prepared with inverted hemipenes; therefore, the fine details, such as the presence of spines and position within the hemipenial apex, were not observable. Based on illustrations by Kluge (1982), the hemibacula of *A. expectatus* exhibit nine spines per element I, these varying in height from 0.18 to 0.26 mm and being laterally compressed and conical, somewhat resembling the feeding apparatus of conodonts (Jones et al., 2012). Although Kluge (1982) illustrated one element per hemipenial lobe (i.e., 2 elements per hemipenis), our μCT data captured only a single element per hemipenis in *A. expectatus* (Figure 2). Similarly, of the three male *A. barbouri*, we examined using μCT, one specimen (AMNH 45795) did not exhibit mineralized hemibacula (Table 1).

The hemipenes of *A. georgeensis*, *A. hechti*, *A. lar*, *A. nelsoni*, and *A. praesignis* (subgenus *Aristelliger*) possess both a mineralized element I and a mineralized element II per hemipenial lobe. In adult males, excluding the ontogenetic series of *A. praesignis*, average lengths of element I ranged from 1.46 to 2.41 mm (Table 1). Element I exhibits a scimitar-shaped morphology in *A. georgeensis*, *A. nelsoni*, and *A. praesignis* and a triangular morphology in *A. hechti* and *A. lar*. Element II exhibits a two-pronged morphology in *A. georgeensis*, *A. nelsoni*, and *A. praesignis*, whereas it exhibits a distally tapered triangular morphology in *A. hechti* and *A. lar* (Figure 2). For the species with the two-pronged element II, average lengths ranged from 1.36 to 2.30 mm for the lateral projection and 1.00–1.28 mm for the medial projection (Table 1). For species with the triangular element II, average lengths ranged from 1.56 to 2.70 mm (Table 1). Cleared-and-stained specimens demonstrate that spines are present on the distal edges of hemibacula of all species belonging to the subgenus *Aristelliger*, although there is variation in their number and in which spines are mineralized (alizarin-positive), alcian-positive, or seemingly unstained. In the case of two specimens (*A. lar* [KU H-228785], *A. hechti* [KU H-228752]), clearing and staining and μCT revealed extensive mineralization in a lambdoidal ("Y")-shaped element situated proximal to the apices of the hemipenes (Figure 2).

Histology of an adult *A. lar* hemipenis reveals hemibacula to be composed of mineralized, densely packed tissue and to be situated centrally in the lobe of each hemipenis, medial to the retractor muscles (Figure 3a–k). Alcian-positive cells are embedded in the densely packed mineralized tissue, primarily in the distal edges of the hemibaculum (Figure 3c–h). In some cases, alcian-positive cells are arranged isogenously (Figure 3f–h). Hemibacula in several sections appear to be hollow and are heavily vascularized in their proximal regions (Figure 3c–e). Hemibacula are covered by a layer of epidermis that often exhibits barb-like shapes on its exposed surface (Figure 3c–i). Proximal portions of the hemibaculum are confluent and merge insensibly with unmineralized dense connective tissue (Figure 3j–k).

3.2 | Hemibacula of *Aristelliger praesignis* through postnatal ontogeny

The postnatal SVLs of *Aristelliger praesignis* examined range from 23 to 100.7 mm (Griffing et al., 2017, 2018). Hemibacula were not

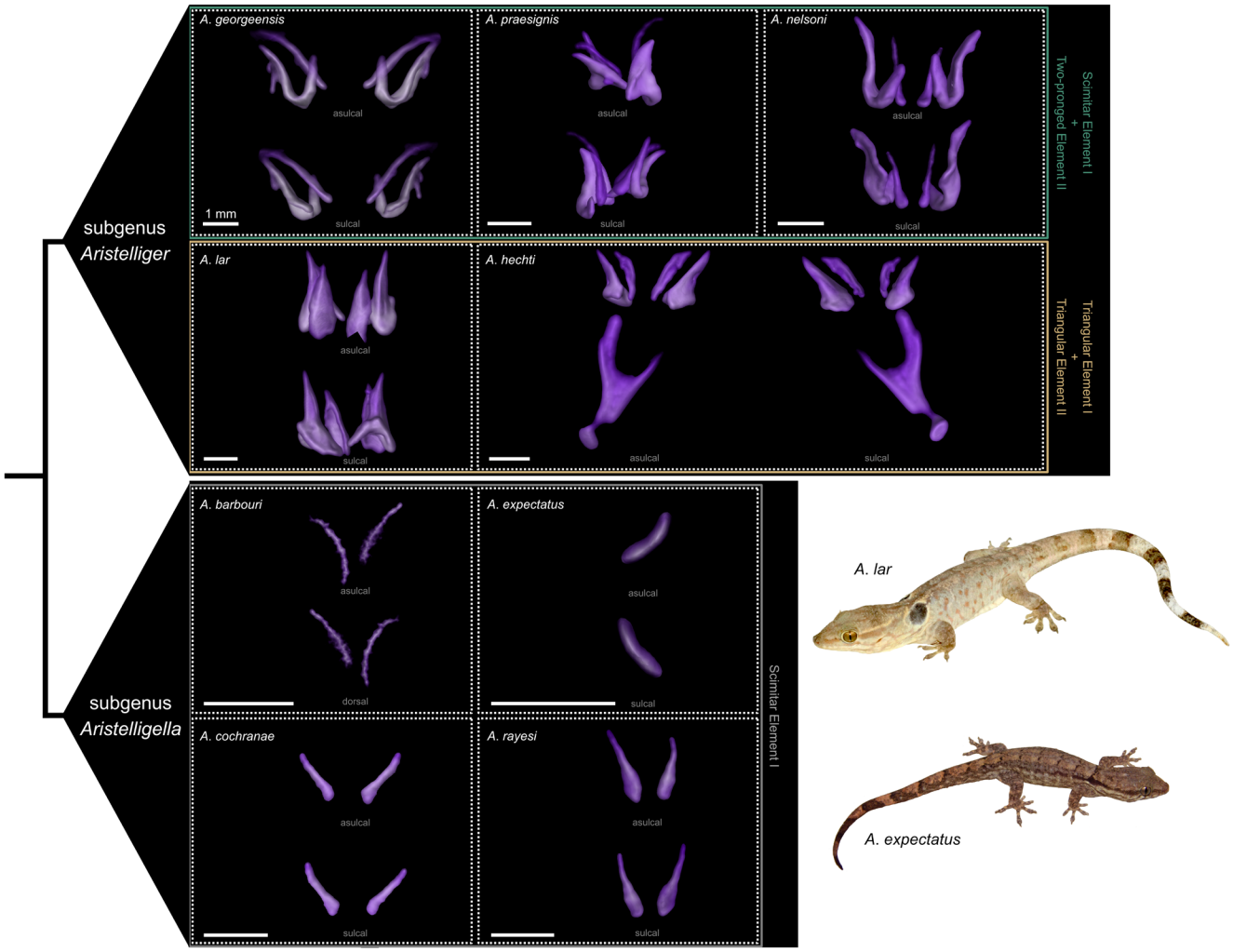

FIGURE 2 Subgenera of *Aristelliger* can be partially defined by their hemibacular characters. μCT hemibacula of the left hemipenis in sulcal and asulcal views of all currently recognized species of *Aristelliger*. Species of the subgenus *Aristelliger* exhibit hemibacular elements I and II and species of the subgenus *Aristelligella* exhibit only hemibaculum element I. Hemibacula are illustrated in purple. Inset bottom right: Representative in-life photographs of a species of each subgenus: *A. lar* and *A. expectatus*.

apparent in the cleared and stained hemipenes of a 52.3 mm SVL individual (MCZ R-194590)—the smallest individual we were able to confidently identify as male (Figure 4). Unmineralized connective tissue precursors of the hemibacula are visible in a 57.9 mm SVL specimen (MCZ R-194581; Figure 4). Mineralization and accumulation of chondroitin sulfate in the spines is underway in the proximal regions of element I and the proximo-lateral portion of element II in a 60.8 mm SVL specimen (MCZ R-194588; Figure 4). By 74.9 mm SVL (MCZ R-194583), the remainder of elements I and II exhibit mineralization and accumulation of chondroitin sulfate in the spines (Figure 4). Beyond this stage, additional mineralization may accrete to the "core" of the hemibaculum in the proximal regions and in the apical spines (Figure 4). Spanning developmental stages, average measurements of element I and element II scale positively with SVL (Figure 5; Table 1). The slopes of log-transformed linear regressions for element I, element II (lateral projection), and element II (medial projection) were 1.24, 1.02, and 1.26, respectively (Figure 5). None of these slopes was significantly different from a slope = 1 (p-values = 0.363 [element I], 0.950 [element II lateral], 0.257 [element II medial]).

4 | DISCUSSION

Our survey reveals that all currently recognized species of *Aristelliger* possess hemibacula and confirms, for the first time, their presence in *A. barbouri*, *A. cochranae*, *A. nelsoni*, *A. hechti*, *A. lar*, and *A. reyesi* (Figure 2). Although hemibaculum element length generally increases with SVL, there is both intra- and interspecific variation (Figure 5; Table 1). Furthermore, element II character states may be useful for *Aristelliger* systematics. The absence of hemibaculum element II characterizes the small-bodied species of *Aristelliger* that constitute the subgenus *Aristelligella* (*A. barbouri*, *A. cochranae*, *A. expectatus*, *A. reyesi*). These hemipenial character states, in tandem with body size differences, and toe pad morphologies, provide further support for the distinct lineages of the subgenera *Aristelligella* and *Aristelliger* (Cloud, 2013; Hecht, 1952;

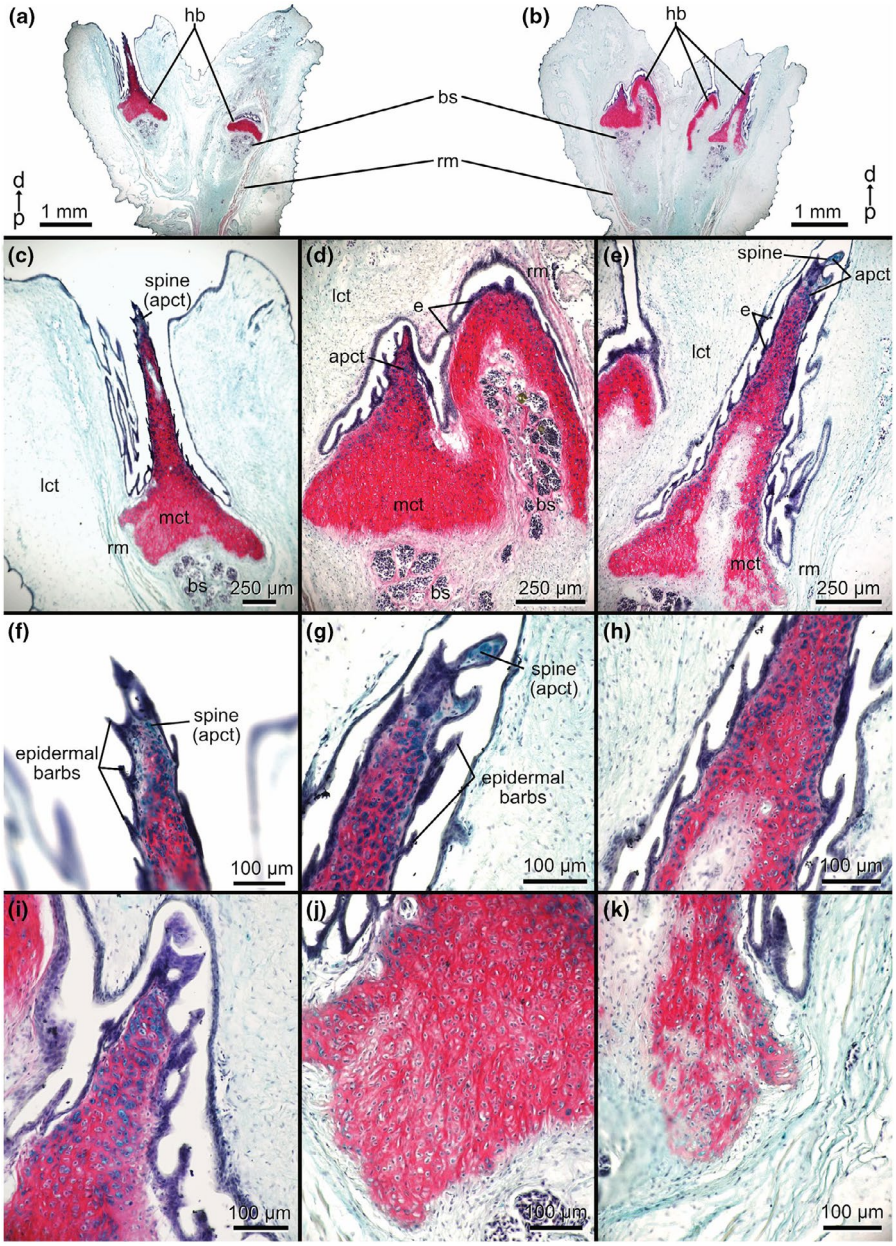

FIGURE 3 Histology of the hemibacula of *Aristelliger lar*. All sections stained with the Hall-Brundt Quadruple Stain. Distal (d) and proximal (p) directions illustrated via a black arrow. (a–b) 4× magnified sections of whole hemipenes. (c–e) 10–20× magnified sections of hemibacula. (f–k) 40× magnified sections of different regions of hemibacula. apct, alcian-positive connective tissue; bs, blood sinuses; e, epidermis; hb, hemibacula; lct, loose connective tissue; mct, mineralized connective tissue; rm., retractor muscle; spine, hemibacular spines.

Noble & Klingel, 1932). Furthermore, when present, element II morphology may prove useful for the systematics of large-bodied *Aristelliger* that constitute the subgenus *Aristelliger* (*A. georgeensis*, *A. hechti*, *A. lar*, *A. nelsoni*, and *A. praesignis*). Two-pronged element II morphology is present in *A. georgeensis*, *A. nelsoni*, and *A. praesignis*. Triangular element II morphology is observed only in *A. hechti* and *A. lar*. The species groupings outlined above correspond to the three clades that have been recovered in previous phylogenetic studies (Cloud, 2013; Keating et al., 2020; Figure 2).

Histological examination of the hemibacula of *A. lar* revealed a dense matrix of mineralized connective tissue (Figure 3). This cell-dense, mineralized tissue exhibiting alcian-positive, spherical cells is somewhat reminiscent of the developing chondroid bone found in *Alligator* skulls (Vickaryous & Hall, 2008). However, its fibrous and cellular characteristics suggest that the hemibacula of *Aristelliger* consist of mineralized tissue, not true bone, similar to the postcloacal bones of geckos (Russell et al., 2016). Kluge (1982) posited that hemibacula do not exhibit an "integumentary coat" (which would be immunologically untenable). We demonstrate that the hemibacula are coated in a thin epidermal layer bearing barbs and are not directly exposed to the external environment when everted (Figure 3). Tissue morphology of the

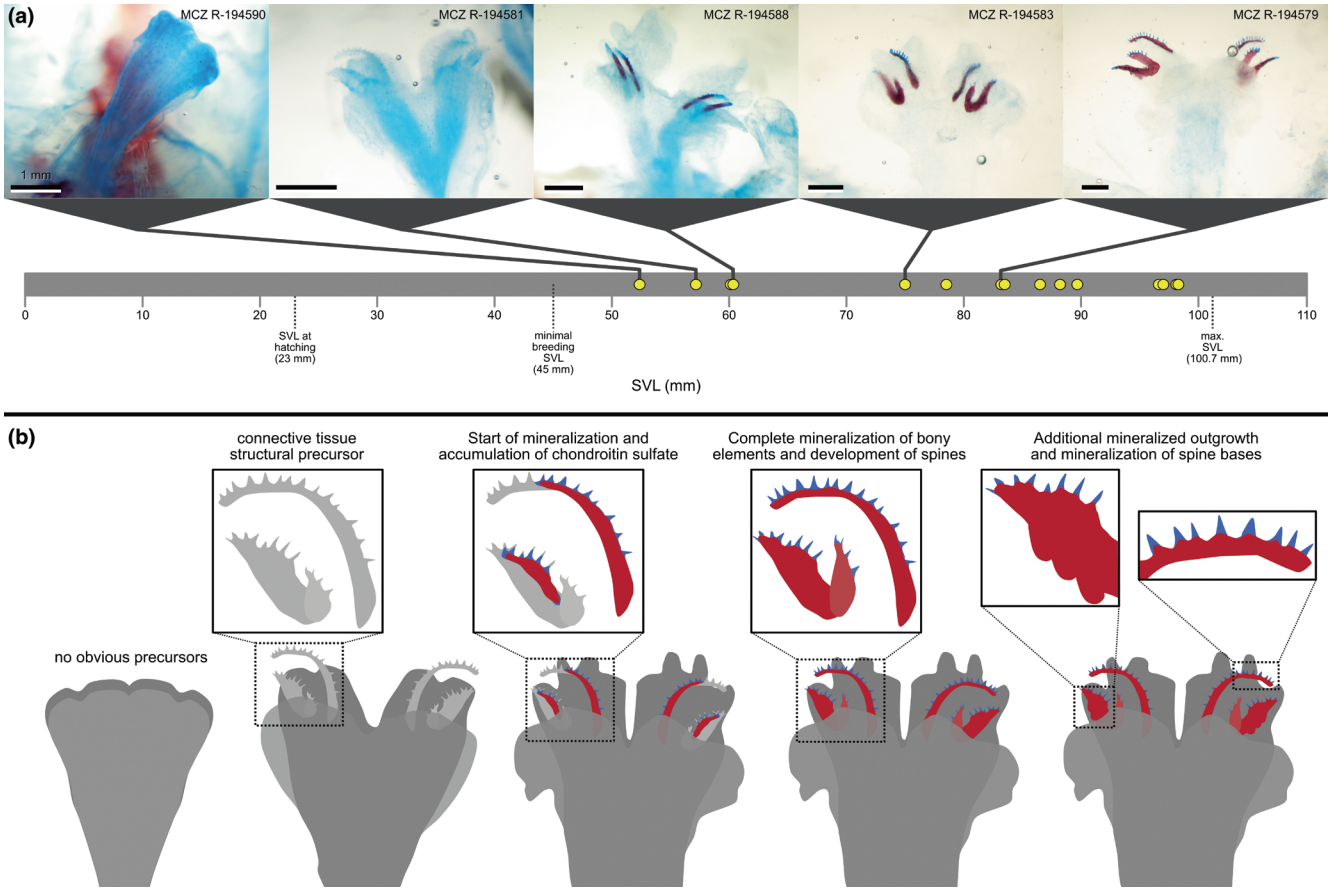

FIGURE 4 Development of hemibacula in a single population of *Aristelliger praesignis*. (a) cleared and stained everted hemipenes of an ontogenetic series of *A. praesignis*. Hemibacula at later ontogenetic stages (larger snout–vent lengths [SVLs]) exhibiting alizarin and alcian staining are positive for mineralized tissue (red) and chondroitin sulfate (dark blue), respectively. Early stages (MCZ R-194590, MCZ R-194581) exhibit soft-tissue overstaining for alcian and likely are not chondroitin sulfate-positive. Yellow points along the SVL continuum (grey bar) correspond to individual specimens that were examined in this study. Scale bars = 1 mm. SVL at hatching, minimum breeding SVL, and maximum SVL acquired from Griffing et al. (2018), Hecht (1952), and Griffing et al. (2017), respectively. (b) Schematic representing how hemibaculum development progresses.

densely packed mineralized tissue and its position directly below the epidermal layer suggest hemibacula are mineralized dermal condensations. Blood sinuses are situated proximal to hemibacula in most sections (Figure 3). Ample blood supply is known to be crucial for the development of mineralized structures like bone (Marenzana & Arnett, 2013) and may be important for the mineralization of hemipenial connective tissue in addition to erectile function. Partially mineralized proximal regions of the hemibacula suggest accretionary mineralization occurs in the proximal direction. Mineralization in these regions may foreshadow further mineralization of connective tissue or ligaments seen as a lambdoidal ("Y")-shaped condensation in our μCT and cleared and stained specimens of *A. lar* and *A. hechti*. Alcian-positive hemibacular spines in cleared and stained specimens were previously interpreted as being cartilaginous (Figure 1(g)). Histology of these presumably cartilaginous regions revealed unexpected tissue morphology. The spherical shape and isogenous organization of alcian-positive cells is similar to, but not exclusive to, hyaline or elastic cartilage (Figure 3(f)–(k)); however, they are embedded in fibrous, mineralized tissue. Furthermore, the alcian-positive cells appear to abut the matrix rather than being segregated by lacunae (Figure 3g). Therefore, we hesitate to ascribe these cells to chondrocytes. Hematoxylin- and eosin-stained histology of the hemibaculum of *Varanus salvator* has revealed portions of the hemipenes exhibiting hyaline cartilage as well as dense connective tissue similar to what we see in the hemibacula of *Aristelliger* (Al-ma'ruf et al., 2021). Although often used as an indicator of cartilage in biological research, due to its affinity for staining chondroitin sulfates, alcian blue also has affinity for other glycosaminoglycans, such as hyaluronic acid, dermatan sulfate, and keratan sulfates found in connective tissue, skin, cartilage, eye tissues, and heart tissue (Schenk & Mowry, 1983). Dense connective tissue with blood sinuses was also observed in the hemipenial armature of lacertid lizards (Arnold, 1986b). Histological investigations of hemipenes are rare (e.g. Al-ma'ruf et al., 2021; Rosenberg, 1967; Sayyadi et al., 2020). It is unknown whether these arrangements of vascularized dense connective tissue are common in squamate hemipenes, but they may be important precursors for mineralized

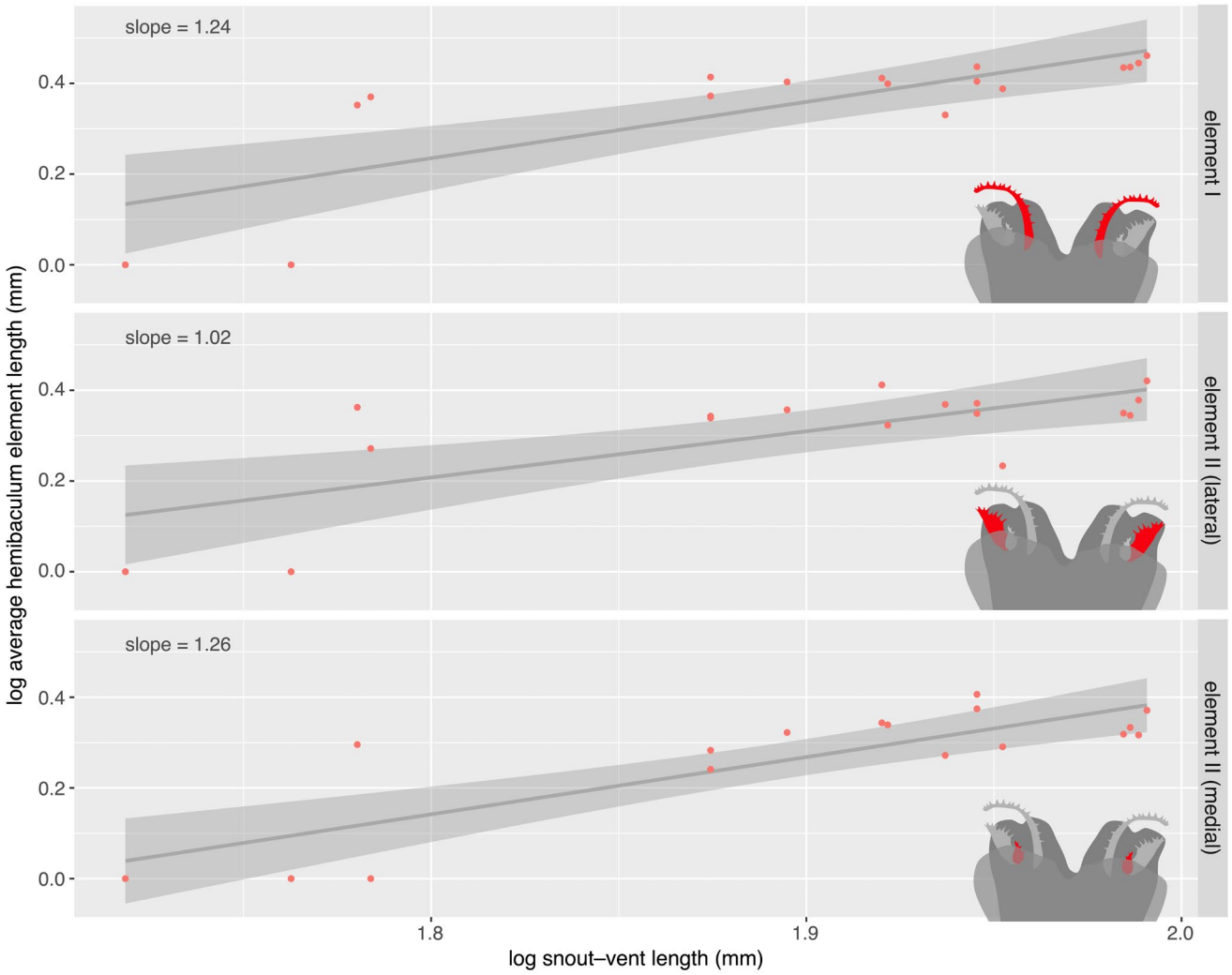

FIGURE 5 Isometric scaling of hemibacula elements in an ontogenetic series of *Aristelliger praesignis*. Each point represents a log-transformed average measurement (average derived from individual hemipenis lobes) from an individual specimen. Respective elements measured are illustrated (red) at the bottom right of each plot.

elements. A more intensive histological investigation of gecko hemipenes, generally, and of *Aristelliger* hemibaculum development, is required to confidently assess the tissue composition of these structures.

Our ontogenetic data gleaned from a single population of *A. praesignis* revealed that hemibacula develop entirely postnatally, originating as non-mineralized connective tissue precursors before eventually mineralizing around 60 mm SVL (Figure 4). The minimum breeding size of *A. praesignis* was estimated by Hecht (1952) to be 45 mm SVL, suggesting that hemibacula do not develop until after the onset of sexual maturity. Interestingly, the bacula of mammals (composed of true bone) are noticeable during late embryonic development and early postnatal development (Smirnov & Tsytsulina, 2003; Yonezawa et al., 2011). Conversely, mineralization of apical ornamentation in snake hemipenes arises at the onset of sexual maturity (Cadle, 2011). Our investigation into developmental allometric scaling of hemibacula in *A. praesignis* revealed an isometric pattern of growth (Figure 5). Previous work revealed that *A. praesignis* exhibits significant male-biased sexual size dimorphism, which is distinct from other sphaerodactylid geckos (Griffing et al., 2018). Generally, traits under sexual selection are phenotypically variable and exhibit positive allometry (Eberhard, 1985). Investigations into baculum diversity in mammalian lineages, including previous work on muskrats and bats, demonstrate positive allometry with body size (e.g. Lüpold et al., 2004; Tasikas et al., 2009). Other mammalian lineages, such as canids, exhibit isometric scaling of bacula and body size (de Latorre & Marshall, 2025). Isometric scaling of baculum size with body size is hypothesized to manifest in species with pre-copulatory selection (Kinahan et al., 2008), which may be the case for *Aristelliger*. However, in our limited ontogenetic series, we were unable to quantify other axes of hemibaculum variation that may be under sexual selection, such as element curvature, number of spines, and rigidity of the hemibacula. A more in-depth characterization using 3D morphometrics, mating biomechanics, female mate choice data, and increased sampling are needed to fully assess the degree to which hemibacula are under sexual selection.

Aristelliger exhibits extremely derived morphologies in comparison to other sphaerodactylid geckos, such as a combination of broad, undivided basal toe pads and asymmetrical distal toe pads, the presence of oil droplets in visual cells, and the most extreme range of sphaerodactylid body sizes (50–135 mm maximum SVL; Bauer & Russell, 1993; Griffing et al., 2018; Röll, 2000; Schwartz & Henderson, 1991). Additionally, *Aristelliger* is one of two sphaerodactylid gecko genera to possess novel parafrontal bones in the supraorbital region of the skull (Bauer & Russell, 1989; Griffing et al., 2018). Parafrontals appear to be peramorphic in origin and also only develop postnatally (Daza et al., 2015; Griffing et al., 2018). Peramorphosis via extended growth phases (i.e., hypermorphosis; de Beer, 1930) results in large sizes and elaborate morphologies when compared to their ancestral form (Alberch et al., 1979; McNamara, 1986). There is no known link between the cranial hyperossification of *Aristelliger* and the presence of hemibacula; however, the occurrence of hyperossification and extreme postnatal mineralization is a trend in other peramorphic lizard taxa, such as *Gekko gecko* (Daza et al., 2015; Laver et al., 2020; Vickaryous et al., 2015) and *Varanus komodoensis* (Maisano et al., 2019; Pavón-Vázquez et al., 2022). Although the genus *Aristelliger* overall is likely peramorphic, the degree of elaboration of hemibacula, similarly to that of parafrontals, appears to be amplified in the large-bodied and derived clade constituting the subgenus *Aristelliger* (Griffing et al., 2018; Hecht, 1952).

The functional significance of squamate hemibacula remains uncertain. Non-mineralized basal spines on the hemipenes of some snakes are used to anchor the hemipenis in the cloaca before "adjustment" and prolong copulation in these limbless squamates (Edgren, 1953; Friesen et al., 2014; Pisani, 1976; Pope, 1941). Calcified spines are also present on the hemipenes of some gymnophthalmid lizards and similar limb-reduced anchoring hypotheses have been proposed to explain their evolution; however, there is no significant association with spine presence and limb reduction in gymnophthalmids (Nunes et al., 2014; Presch, 1978). Regardless, Nunes et al. (2014) posited hemipenial spines may be used to prolong copulation or mechanically moving scales in the cloacal region. Kluge (1982) suggested that the hemibacula of *Aristelliger* are "too weakly developed" to serve as hemipenial anchors and proposed several alternative hypotheses to explain the unique apical position and denticulate ornamentation of these structures. Potential (not mutually exclusive) functions suggested were: disturbance of female seminal receptacles in an attempt to remove the sperm of other individuals; improvement of female receptivity; provisioning of the male with sensory feedback with which to regulate or terminate copulation (Crews, 1978; Cuellar, 1966). Notwithstanding, hemipenial anchorage may be important for *Aristelliger* because it exhibits regional integumentary loss (Bauer & Russell, 1992; Díaz & Hedges, 2009). Since male geckos generally stabilize themselves during copulation by biting the nape of the female's neck, hemibacula may provide added stability if the female's integument is ruptured while mating or may obviate the need for sustained nape biting.

Functional studies of mammalian reproduction have posited several functions for bacula, including support and preventing urethral collapse (e.g., Herdina et al., 2015), prolonging intromission (e.g., Dixson et al., 2004), stimulating the release of prolactin for sperm competition (André et al., 2021) and stimulating ovulation (e.g., Greenwald, 1956). In particular, recent work suggests that short-term inflammation and copulatory wounding of the female reproductive tract can be beneficial for inducing ovulation and promoting embryo implantation (Brennan et al., 2024; Griffith et al., 2017). It is possible that the jagged hemibacula of *Aristelliger* may abrade the reproductive tract, thereby creating a similar ovulatory response. However, a possible constraint on the elaboration of hemibacular spines and their jagged shape is the ability to safely invert hemipenes without injuring the male. Until a detailed investigation of *Aristelliger* female reproductive anatomy and copulation experiments are conducted, the function of hemibacula remains speculative.

AUTHOR CONTRIBUTIONS

AHG and AMB conceived and designed the study. AHG, DJP, JCD, JDD, and TG acquired data. AHG, DJP, APR, and AMB analyzed and interpreted the data. AHG, DJP, JDD, TG, APR, and AMB drafted the manuscript. All authors approved the final version of this article.

ACKNOWLEDGEMENTS

We thank José Rosado (MCZ), Carol Spencer (MVZ), Luke Welton (KU), Robert Wilson (NMNH), Addison Wynn (NMNH) and David Blackburn (UF) for access to museum specimens. Additional thanks go to Arianna Kuhn and Jeff Weinell for photographing some AMNH specimens. Field collection of *Aristelliger praesignis* would not have been possible without permission and assistance from the Jamaican National Environment & Planning Agency (NEPA), Byron Wilson and Michael Rowe. We thank Matt Vickaryous for his thoughtful insights concerning mineralized tissue histology. This research was supported by the Villanova University Department of Biology and the Gerald E. Lemole endowed Chair Fund. CT scanning was performed as part of the openVertebrate (oVert) Thematic Collections Network (National Science Foundation DBI 1701714 to Edward Stanley). This work was made possible in part by the National Science Foundation (DBI 2209090 to AHG, DBI 2109344 to DJP). Finally, we thank three anonymous reviewers who provided valuable feedback on an earlier version of this manuscript.

CONFLICT OF INTEREST STATEMENT

The authors declare no conflicts of interest.

DATA AVAILABILITY STATEMENT

Data used in this manuscript are freely available from MorphoSource (Project ID: 0000C1044; https://doi.org/10.17602/M2/M116838, https://doi.org/10.17602/M2/M116852, https://doi.org/10.17602/M2/M116855, https://doi.org/10.17602/M2/M116828, https://doi.org/10.17602/M2/M116850, https://doi.org/10.17602/M2/M116832, https://doi.org/10.17602/M2/M116790, https://doi.org/10.17602/M2/M116841, https://doi.org/10.17602/M2/M116853, https://doi.org/10.17602/M2/M116848, https://doi.org/10.17602/M2/M116835) and FigShare (https://doi.org/10.6084/m9.figshare.29043092).

ORCID

Aaron H. Griffing https://orcid.org/0000-0001-8441-1330
Daniel J. Paluh https://orcid.org/0000-0003-3506-2669
Juan D. Daza https://orcid.org/0000-0002-5651-0240
Tony Gamble https://orcid.org/0000-0002-0204-8003
Anthony P. Russell https://orcid.org/0000-0001-6659-6765
Aaron M. Bauer https://orcid.org/0000-0001-6839-8025

REFERENCES

Alberch, P., Gould, S.J., Oster, G.F. & Wake, D.B. (1979) Size and shape in ontogeny and phylogeny. *Paleobiology*, 5, 296–317.

Al-ma'ruf, A.Y., Sari, R.P., Mustofa, I., Utama, S., Anwar, C., Mafruschati, M. et al. (2021) Morphology and histology of paryphasmata and hemibaculum of *Varanus salvator* based on sexual maturity. *Open Veterinary Journal*, 11, 330–336.

André, G.I., Firman, R.C. & Simmons, L.W. (2021) The effect of baculum shape and mating behavior on mating-induced prolactin release in female house mice. *Behavioral Ecology*, 32, 1192–1201.

Arnold, E.N. (1986a) Why copulatory organs provide so many useful taxonomic characters: the origin and maintenance of hemipenial differences in lacertid lizards (Reptilia: Lacertidae). *Biological Journal of the Linnean Society*, 29, 263–281.

Arnold, E.N. (1986b) The hemipenis of lacertid lizards (Reptilia: Lacertidae): structure, variation and systematic implications. *Journal of Natural History*, 20, 1221–1257.

Bauer, A.M. (1986) Systematics, biogeography and evolutionary morphology of the Carphodactylini (Reptilia: Gekkonidae). Ph.D. thesis, University of California at Berkeley, Berkeley, California USA.

Bauer, A.M. & Russell, A.P. (1989) Supraorbital ossifications in geckos (Reptilia: Gekkonidae). *Canadian Journal of Zoology*, 67, 678–684.

Bauer, A.M. & Russell, A.P. (1992) The evolutionary significance of regional integumentary loss in Island geckos: a complement to caudal autotomy. *Ethology Ecology & Evolution*, 4, 343–358.

Bauer, A.M. & Russell, A.P. (1993) *Aristelliger*. *Catalogue of American Amphibians and Reptiles*, 565, 1–4.

Böhme, W. (1988) Zur Genitalmorphologie der Sauria: Funktionelle und stammesgeschichtliche Aspekte. *Bonner Zoologische Monographien*, 27, 1–176.

Branch, W.R. (1982) Hemipeneal morphology of platynotan lizards. *Journal of Herpetology*, 16, 16–38.

Brennan, I.G. & Bauer, A.M. (2017) Notes on hemipenial morphology and its implications in the Pygopodidae Boulenger, 1884. *Bonn Zoological Bulletin*, 66, 15–28.

Brennan, P.L.R., Purdy, S. & Bacon, S.J. (2024) Intra-horn insemination in the alpaca *Vicugna pacos*: Copulatory wounding and deep sperm deposition. *PLoS One*, 19, e0295882.

Cadle, J.E. (2011) Hemipenial morphology in the north American snake genus *Phyllorhynchus* (Serpentes: Colubridae), with a review and comparisons with natricid hemipenes. *Zootaxa*, 3092, 1–25.

Card, W. & Kluge, A.G. (1995) Hemipeneal skeleton and varanid lizard systematics. *Journal of Herpetology*, 29, 275–280.

Cloud, T.L. (2013) Cryptic diversity, evolution, and biogeography of Caribbean croaking geckos (Genus: *Aristelliger*). Master's thesis, Pennsylvania State University, University Park, Pennsylvania USA.

Conroy, C.J., Papenfuss, T., Parker, J. & Hahn, N.E. (2009) Use of tricaine methanesulfonate (MS222) for euthaniasia of reptiles. *Journal of the American Association for Laboratory Animal Science*, 48, 28–32.

Cope, E.D. (1896) On the hemipenes of the Sauria. *Proceedings of the Academy of Natural Sciences of Philadelphia*, 48, 461–467.

Crews, D. (1978) Integration of internal and external stimuli in the regulation of lizard reproduction. In: Greenberg, N. & MacLean, P.D. (Eds.) *Behavior and neurology of lizards*. Maryland: National Institute of Mental Health, pp. 149–171.

Cuellar, O. (1966) Oviducal anatomy and sperm storage structures in lizards. *Journal of Morphology*, 119, 7–20.

Das, M. & Purkayastha, J. (2012) Insight into hemipenial morphology of five species of *Hemidactylus* Oken, 1817 (Reptilia: Gekkonidae) of Guwahati, Assam, India. *Hamadryad*, 36, 32–37.

Daza, J.D., Mapps, A.A., Lewis, P.J., Thies, M.L. & Bauer, A.M. (2015) Peramorphic traits in the tokay gecko skull. *Journal of Morphology*, 276, 915–928.

de Beer, G.R. (1930) *Embryology and evolution*. Oxford: Clarendon.

de Latorre, D.V. & Marshall, C.R. (2025) Evolutionary allometry of the canid baculum (Carnivora: Mammalia). *Biological Journal of the Linnean Society*, 144, blae048.

De Lima, A.K.S., Paschoaletto, I.P., Pinho, L.D.O., Benmamman, P. & Klaczko, J. (2019) Are hemipenial traits under sexual selection in *Tropidurus* lizards? Hemipenial development, male and female genital morphology, allometry and coevolution in *Tropidurus torquatus* (Squamata: Tropiduridae). *PLoS One*, 14, e0219053.

Díaz, L.M. & Hedges, S.B. (2009) First record of the genus *Aristelliger* (Squamata: Sphaerodactylidae) in Cuba, with description of a new species. *Zootaxa*, 2028, 31–40.

Dixson, A., Nyholt, J. & Anderson, M. (2004) A positive relationship between baculum length and prolonged intromission patterns in mammals. *Acta Zoologica Sinica*, 50, 490–503.

Dowling, H.G. & Savage, J.M. (1960) A guide to the snake hemipenis: a survey of basic structure and systematic characteristics. *Zoologica*, 45, 17–28.

Eberhard, W.G. (1985) *Sexual selection and animal genitalia*. Cambridge: Harvard University Press.

Edgren, R.A. (1953) Copulatory adjustment in snakes and its evolutionary implications. *Copeia*, 3, 162–164.

Friesen, C.R., Uhrig, E.J., Squire, M.K., Mason, R.T. & Brennan, P.L.R. (2014) Sexual conflict over mating in red-sided garter snakes (*Thamnophis sirtalis*) as indicated by experimental manipulation of genitalia. *Proceedings of the Royal Society B: Biological Sciences*, 281, 20132694.

Glaw, F., Koscuh, J., Henkel, F.-W., Sound, P. & Böhme, W. (2006) Genetic and morphological variation of the leaf-tailed gecko *Uroplatus fimbriatus* from Madagascar, with description of a new giant species. *Salamandra*, 42, 129–144.

Glaw, F., Vences, M., Ziegler, T., Böhme, W. & Köhler, J. (1999) Specific distinctness and biogeography of the dwarf chameleons *Brookesia minima*, *B. peyrierasi* and *B. tuberculata* (Reptilia: Chamaeleonidae): evidence from hemipenial and external morphology. *Journal of Zoology*, 247, 225–238.

Greenwald, G.S. (1956) The reproductive cycle of the field mouse (*Microtus californicus*). *Journal of Mammalogy*, 37, 213–222.

Griffing, A.H., Daza, J.D., DeBoer, J.C. & Bauer, A.M. (2018) Developmental osteology of the parafrontal bones of the Sphaerodactylidae. *The Anatomical Record*, 301, 581–606.

Griffing, A.H., DeBoer, J.C., Campbell, P.D., Wilson, B.S. & Bauer, A.M. (2017) *Aristelliger praesignis* (Jamaican croaking lizard). Maximum size. *Herpetological Review*, 48, 184–185.

Griffith, O.W., Chavan, A.R., Protopapas, S., Maziarz, J., Romero, R. & Wagner, G.P. (2017) Embryo implantation evolved from an ancestral inflammatory attachment reaction. *Proceedings of the National Academy of Sciences of the United States of America*, 114, E6566–E6575.

Hall, B.K. (1986) The role of movement and tissue interactions in the development and growth of bone and secondary cartilage in the clavicle of the embryonic chick. *Journal of Embryology and Experimental Morphology*, 93, 133–152.

Hanken, J. & Wassersug, R.J. (1981) The visible skeleton. *Functional Photography*, 16, 22–26.

Hecht, M.K. (1952) Natural selection in the lizard genus *Aristelliger*. *Evolution*, 6, 112–124.

Herdina, A.N., Kelly, D.A., Jahelková, H., Lina, P.H.C., Horáček, I. & Metscher, B.D. (2015) Testing hypotheses of bat baculum function

with 3D models derived from micorCT. *Journal of Anatomy*, 226, 229–239.
Jahed-Haghshenas, N. & Hojati, V. (2015) The male reproductive cycle of the Bedriaga's plate-tailed gecko, *Teratoscincus bedriagai* in Iran. *Iranian Journal of Animal Biosystematics*, 11, 7–16.
Jones, D., Evans, A.R., Siu, K.K.W., Rayfield, E.J. & Donoghue, P.C.J. (2012) The sharpest tools in the box? Quantitative analysis of conodont element functional morphology. *Proceedings of the Royal Society B: Biological Sciences*, 279, 2849–2854.
Keating, S.E., Griffing, A.H., Nielsen, S.V., Scantlebury, D.P. & Gamble, T. (2020) Conserved ZZ/ZW sex chromosomes in Caribbean croaking geckos (*Aristelliger*: Sphaerodactylidae). *Journal of Evolutionary Biology*, 33, 1316–1326.
Keogh, J.S. (1999) Evolutionary implications of hemipenial morphology in the terrestrial Australian elapid snakes. *Zoological Journal of the Linnean Society*, 1999, 239–278.
Kerney, R., Wassersug, R. & Hall, B.K. (2009) Skeletal advance and arrest in giant non-metamorphosing African clawed frog tadpoles (*Xenopus laevis*: Daudin). *Journal of Anatomy*, 216, 132–143.
Kinahan, A.A., Bennett, N.C., Belton, L.E. & Bateman, P.W. (2008) Do mating strategies determine genital allometry in African mole rats (Bathyergidae). *Journal of Zoology*, 274, 312–317.
Kluge, A.G. (1982) Cloacal bones and sacs as evidence of gekkonoid lizard relationships. *Herpetologica*, 38, 348–355.
Köhler, J., Hahn, M. & Köhler, G. (2012) Divergent evolution of hemipenial morphology in two cryptic species of mainland anoles related to *Anolis polylepis*. *Salamandra*, 48, 1–11.
Laver, R.J., Morales, C.H., Heinicke, M.P., Gamble, T., Longoria, K., Bauer, A.M. et al. (2020) The development of cephalic armor in the tokay gecko (Squamata: Gekkonidae: *Gekko gecko*). *Journal of Morphology*, 281, 213–228.
Lindahl, U. & Hook, M. (1978) Glycosaminoglycans and their binding to biological macromolecules. *Annual Review of Biochemistry*, 47, 385–417.
Lüpold, S., McElligott, A.G. & Hsoken, D.J. (2004) Bat genitalia: Allometry, variation and good genes. *Biological Journal of the Linnean Society*, 83, 497–507.
Maisano, J.A., Laduc, T.J., Bell, C.J. & Barber, D. (2019) The cephalic osteoderms of *Varanus komodoensis* as revealed by high-resolution X-ray computed tomography. *The Anatomical Record*, 302, 1675–1680.
Marenzana, M. & Arnett, T.R. (2013) The key role of the blood supply to bone. *Bone Research*, 3, 203–215.
McNamara, K.J. (1986) A guide to the nomenclature of heterochrony. *Journal of Paleontology*, 60, 4–13.
Noble, G.K. & Klingel, G.C. (1932) The reptiles of great Inagua Island, British West Indies. *American Museum Novitates*, 539, 1–25.
Nunes, P.M.S., Curcio, F.F., Roscito, J.G. & Rodrigues, M.T. (2014) Are hemipenial spines related to limb reduction? A spiny discussion focused on gymnophthalmid lizards (Squamata: Gymnophthalmidae). *The Anatomical Record*, 297, 482–495.
Pavón-Vázquez, C.J., Esquerré, D. & Keogh, J.S. (2022) Ontogenetic drivers of morphological evolution in monitor lizards and allies (Squamata: Paleoanguimorpha), a clade with extreme body size disparity. *BMC Ecology and Evolution*, 22, 15.
Pisani, G.R. (1976) Comments on the courtship and mating mechanisms of *Thamnophis* (Reptilia, Serpentes, Colubridae). *Journal of Herpetology*, 10, 139–142.
Pope, C.H. (1941) Copulatory adjustment in snakes. *Field Museum of Natural History—Zoological Series*, 24, 249–252.
Presch, W. (1978) Descriptions of the hemipenial morphology in eight species of microteiid lizards (family Teiidae, subfamily Gymnophthalminae). *Herpetologica*, 34, 108–112.
Röll, B. (2000) Gecko vision—visual cells, evolution, and ecological constraints. *Journal of Neurocytology*, 29, 471–484.
Rosenberg, H.I. (1967) Hemipenial morphology of some amphisbaenids (Amphisbaenia: Reptilia). *Copeia*, 1967, 349–361.
Rösler, H. & Böhme, W. (2006) Peculiarities of the hemipenes of the gekkonid lizard genera *Aristelliger* Cope, 1861 and *Uroplatus* Duméril, 1806. In: Vences, M., Köhler, J., Ziegler, T. & Böhme, W. (Eds.) *Herpetologia Bonnensis II, proceedings of the 13th congress of the Societas Europaea Herpetologica*. Bonn, Germany: Societas Europaea Herpetologica, pp. 121–124.
Russell, A.P. (1977) Comments concerning postcloacal bones in geckos (Reptilia: Gekkonidae). *Canadian Journal of Zoology*, 55, 1201–1205.
Russell, A.P., Vickaryous, M.K. & Bauer, A.M. (2016) The phylogenetic distributions, anatomy and histology of the post-cloacal bones and adnexa of geckos. *Journal of Morphology*, 277, 264–277.
Sayyadi, F., Rastegar-Pouyani, N., Azadbakht, M. & Chehri, K. (2020) Comparative morphology and histology of the hemipeneal structure of *Laudakia nupta* (De Filippi, 1843) and *Paralaudakia caucasia* (Eichwald, 1843). *Iranian Journal of Animal Biosystematics*, 16, 1–10.
Schenk, E.A. & Mowry, R.W. (1983) Alcian blue: comments on some of its uses and usefulness as a stain for acid mucopolysaccharides (glycosaminoglycans). *Journal of Histotechnology*, 6, 65–69.
Schindelin, J., Arganda-Carreras, I., Frise, E., Kaynig, V., Longair, M., Pietzsch, T. et al. (2012) Fiji: an open-source platform for biological-image analysis. *Nature Methods*, 9, 676–682.
Schwartz, A. & Henderson, R.W. (1991) *Amphibians and reptiles of the West Indies: descriptions, distributions, and natural history*. Gainesville: University Press of Florida.
Shea, G.M. & Reddacliff, G.L. (1986) Ossifications in the hemipenes of varanids. *Journal of Herpetology*, 20, 566–568.
Simmons, J.E. (2015) *Herpetological collecting and collections management*, Third edition. Salt Lake City: Society for the Study of Amphibians and Reptiles.
Smirnov, D.G. & Tsytsulina, K. (2003) The ontogeny of the baculum in *Nyctalus noctule* and *Vespertilio murinus* (Chiroptera: Vespertilionidae). *Acta Chiropterologica*, 5, 117–123.
Smith, M.A. (1935) *The fauna of British India including Ceylon and Burma and adjacent islands. Reptilia and Amphibia. Vol. 2. Sauria*. London: Taylor and Francis.
Tasikas, D.E., Fairn, E.R., Laurence, S. & Schulte-Hostedde, A.I. (2009) Baculum variation and allometry in the muskrat (*Ondatra zibethicus*): a case for sexual selection. *Evolutionary Ecology*, 23, 223–232.
Theoharides, T.C., Patra, P., Boucher, W., Letourneau, R., Kempuraj, D., Chiang, G. et al. (2000) Chondroitin sulphate inhibits connective tissue mast cells. *British Journal of Pharmacology*, 131, 1039–1049.
Vickaryous, M.K. & Hall, B.K. (2008) Development of the dermal skeleton in *Alligator mississippiensis* (Archosauria, Crocodylia) with comments on the homology of osteoderms. *Journal of Morphology*, 269, 398–422.
Vickaryous, M.K., Meldrum, G. & Russell, A.P. (2015) Armored geckos: a histological investigation of osteoderm development in *Tarentola* (Phyllodactylidae) and *Gekko* (Gekkonidae) with comments on their regeneration and inferred function. *Journal of Morphology*, 276, 1345–1357.
Wassersug, R.J. (1976) A procedure for differential staining of cartilage and bone in whole formalin-fixed vertebrates. *Biotechnic and Histochemistry*, 51, 131–134.
Werner, Y.L. (1988) Are hemipenial "ossifications" of Gekkonidae and Varanidae ossified? *Israel Journal of Zoology*, 35, 99–100.
Yonezawa, T., Higashi, M., Yoshioka, K. & Mutoh, K.-I. (2011) Distribution of aromatase and sex steroid receptors in the baculum during rat life cycle: effects of estrogen during the early development of the baculum. *Biology of Reproduction*, 85, 105–112.

How to cite this article: Griffing, A.H., Paluh, D.J., DeBoer, J.C., Daza, J.D., Gamble, T., Russell, A.P. et al. (2025) Diversity and development of the hemibacula of croaking geckos (Sphaerodactylidae: *Aristelliger*). *Journal of Anatomy*, 247, 1145–1156. Available from: https://doi.org/10.1111/joa.70009